### THE CHEMICAL RECORD

# Crystalline, Highly Oriented MOF Thin Film: the Fabrication and Application

Zhihua Fu and Gang Xu\*[a]

Abstract: The thin film of metal-organic frameworks (MOFs) is a rapidly developing research area which has tremendous potential applications in many fields. One of the major challenges in this area is to fabricate MOF thin film with good crystallinity, high orientation and well-controlled thickness. In order to address this challenge, different appealing approaches have been studied intensively. Among various oriented MOF films, many efforts have also been devoted to developing novel properties and broad applications, such as in gas separator, thermoelectric, storage medium and photovoltaics. As a result, there has been a large demand for fundamental studies that can provide guidance and experimental data for further applications. In this account, we intend to present an overview of current synthetic methods for fabricating oriented crystalline MOF thin film and bring some updated applications. We give our perspective on the background, preparation and applications that led to the developments in this area and discuss the opportunities and challenges of using crystalline, highly oriented MOF thin film.

**Keywords:** metal-organic frameworks, thin film, orientation, preparation, application

### 1. Introduction

Metal-organic frameworks (MOFs),<sup>[1–5]</sup> also well-known porous coordination polymers (PCPs), are crystalline polymeric microporous inorganic-organic hybrid materials composed of metal ions bridged by organic ligands. Owing to the uniform pores and high designability in the frameworks, MOFs have been used and studied for wide range of potential applications, such as gas storage and separation,<sup>[6–8]</sup> chemical sensing,<sup>[9]</sup> catalysis,<sup>[10]</sup> drug release,<sup>[11]</sup> electron (proton) conduction<sup>[12,13]</sup> and so on. Numerous applications of MOFs materials require them in thin film forms, and thus in recent years the researches on thin films of MOFs become a rapidly evolving field.<sup>[14–16]</sup>

It is not difficult to envision the use of MOFs thin films for applications in gas adsorption/separation, sensors, photo-

\_\_\_\_

[a] Dr. Z. Fu, Prof. G. Xu State Key Laboratory of Structural Chemistry Fujian Institute of Research on the Structure of Matter, Chinese Academy of Sciences Fuzhou 350052 (P.R. China) E-mail: gxu@fjirsm.ac.cn voltaics, energy storage and electronic devices. Although these topics have been initiated, the studies on these emerging fields present an increasingly developing and ever-broadening trend. Examples of oriented MOFs thin films suggest intriguing possibilities as gas separator, field-effect transistors (FETs), thermoelectric, and solar cell as well. Thus, investigations of the oriented MOFs thin films and their functionalized devices can provide guidance and experimental data for the future research and bring benefits to the practical applications in nano-devices.

A variety of techniques have been developed for MOFs thin film fabrication, such as seeded growth, dip coating, electrochemically and liquid phase epitaxy. Most these methods produce polycrystalline films which typically place MOF micro-particles on a substrate randomly with badly controlled thickness in the micrometer grade. Only a few methods can get crystalline MOF thin film that has high orientation, precisely adjustable thickness and epitaxial growth on a substrate. The first example of oriented growth of MOF thin film might be Cu<sub>3</sub>(BTC)<sub>2</sub>(H<sub>2</sub>O)<sub>3</sub>•xH<sub>2</sub>O, which was reported by Biemmi in 2007. This film shows a preferred crystal orientation that can be tunable with functionalized self-assembled monolayers (SAMs) by direct

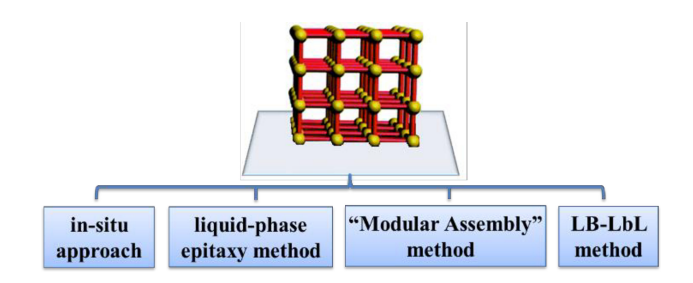
growth/deposition from solvothermal mother solutions. After that, Zacher<sup>[18]</sup> showed the surface selective and oriented growth of Cu<sub>3</sub>(BTC)<sub>2</sub> on SAMs-functionalized SiO<sub>2</sub>/Sisubstrates, as well as on c-plane sapphire surfaces. Soon after, a landmark research was reported by Shekhah and coworkers in 2007 where the controlled and oriented Cu<sub>3</sub>(BTC)<sub>2</sub> thin films were realized by step-by-step route (also called liquid phase epitaxy method).<sup>[19]</sup> In 2010, a highly crystalline oriented MOF thin film, NAFS-1, was achieved by Makiura and coworkers using the Langmuir-Blodgett layer-by-layer (LB-LbL) technique.<sup>[20]</sup> Thereafter, Xu and coworkers developed a new technique known as "modular assembly" method for fabrication of the oriented MOF thin film from nanostructured building blocks in 2012.<sup>[21]</sup>

Although a number of reviews on MOF thin films have been published, [22-29]] new fabrication methods and applications of MOF thin films, especially oriented MOF thin films have emerged continuously in recent years. So, it is necessary to present an overview of recent progress in this field. The mentioned examples in this review are based on the available literature until July 2016. In this review, we firstly describe the fabrication methods of the crystalline and oriented MOF thin films. Then, we review the fields with respect to the properties and applications based on the available literature. Finally, we propose an encouraging outlook with the objective to stimulate the development and implementation of MOFs for nano-devices.

## 2. Methods for Fabrication of Oriented MOF Thin Film

As mentioned in the introduction part, the importance of MOF thin film has triggered the development of a number of different approaches for fabricating it on solid substrates.<sup>[14]</sup>

Among them, methods for synthesizing oriented MOF films are grouped into four categories (Scheme 1) and discussed with selected examples.



Scheme 1. The methods for the fabrication of oriented MOF thin film.

### 2.1. In-situ Deposition of MOFs on a Modified Substrate

This straightforward approach is employed in the successful preparation of various well-defined MOF thin films. Based on this conventional process, an organic SAMs modified substrate is placed into the Teflon autoclave during solvothermal reaction. The SAMs layer is an ultrathin organic layer that assemble spontaneously on surfaces with a well-defined molecular arrangement. The MOFs thin film with different orientation can be fabricated on the substrate in a controlled way by means of varying functional head group of the SAMs.

Biemmi et. al.<sup>[17]</sup> and Zacher et. al.<sup>[18]</sup> almost simultaneously reported the HKUST-1 thin film by utilizing the substrates functionalized by -COOH and -OH terminal SAMs. The results show a remarkable surface selectivity and provide an oriented growth mode on the SAMs functionalized substrate. Bein and coworkers had extended this in-situ synthesis approach to several other MOFs: Fe-MIL-88B,<sup>[30–32]</sup> Fe-MIL-88B-NH<sub>2</sub><sup>[32]</sup> and CAU-1.<sup>[33]</sup> Very recently, Shekhah et. al. developed this method with a new MOF: rho-ZMOF-



Zhihua Fu received his Ph.D. in Organic Chemistry at Zhengzhou University in 2014. Then he worked in the Fujian Institute of Research on the Structure of Matter (FJIRSM), Chinese Academy of Sciences (CAS) as a research assistant. His current research interests are MOF thin films and their electrical properties.



Gang Xu received his Ph.D. in 2008 at FJIRSM, CAS. Then he worked as post-doctoral fellows at COSDAF in City University of Hong Kong (Hong Kong), University of Regensburg (Alexander von Humboldt fellowship, Germany) and Kyoto University (JSPS fellowship, Japan) in sequence. In 2013, he joined FJIRSM and undertook his independent research as a PI. His research interests focus on the surface / interfacial coordination chemistry of materials and the related electrical devices.

1,<sup>[34]</sup> which was the first highly oriented zeolite-like MOF thin film with rho topology.

By this method, crystalline films with micrometer thickness can be fabricated on a wide variety of substrates (oxide wafers, metal slices, textiles or fibers, and even porous alumina in some cases). Importantly, the orientation of MOF thin film can be tuned by the surface modification on the substrate. Taking the growth of HKUST-1 demonstrated by Biemmiet et. al. [17] as an example, the gold slides functionalized SAMs terminated by -COOH, -OH and -Me group are placed into a clear pre-prepared HKUST-1 filtrated mother solution (lying face down or vertical is better to avoid sedimentation), and the thin films are grown gradually at room temperature in glass reactor with long immersion time. Certain crystallographic directions of HKUST-1 thin film can be induced by using different SAMs terminated surfaces, in which the [100] direction is observed on -COOH terminated substrate and [111] direction is showed on the -OH terminated substrate (Figure 1).

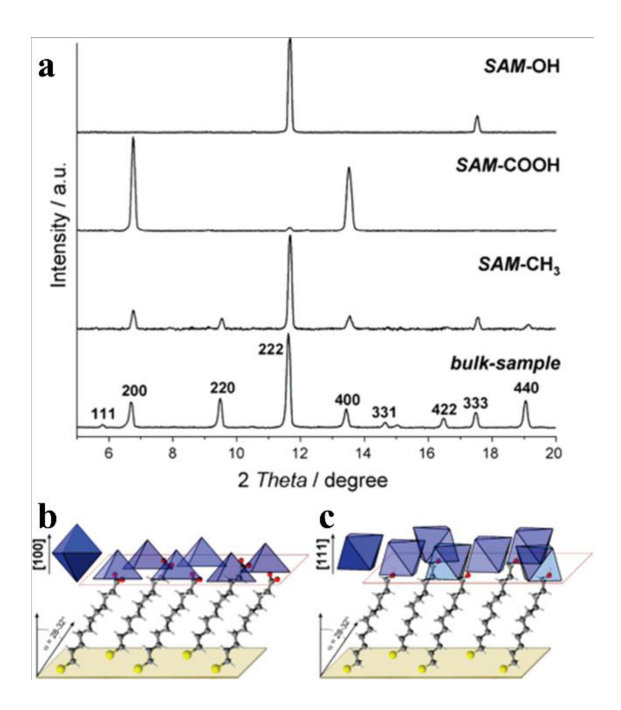


**Figure 1.** (a) X-ray diffraction patterns of Cu<sub>3</sub>(BTC)<sub>2</sub> thin films on functionalized gold surfaces. Bottom: Schematic illustrations of oriented growth of HKUST-1 nanocrystals controlled via surface functionalization: (b) on an 11-mercaptoundecanoic acid SAMs, and (c) on 11-mercaptoundecanol-modified gold surfaces. <sup>[17]</sup> Copyright 2007, American Chemical Society.

This in-situ crystallization approach is straight-forward and powerful for MOF thin film preparation, but there are still inevitable shortcomings in this method. For example, preparation of MOF thin film needs a long and complicated preparation procedure. Typically, it needs a few days with

several heating steps in the pre-preparation steps and elaborate control over the processes of MOF nucleation and growth is also required. Moreover, surface-functionalized substrates also limit their further application. Many SAMs on substrates are temperature sensitive and may fall off at high temperature. Furthermore, the MOF thin films obtained by this method usually show a rough surface and poor morphology. The thickness of films is hard to control, and especially the nano-scale thin films are scarcely possible to prepare using this method.

### 2.2. Liquid-phase Epitaxy Methods

The liquid-phase epitaxy (LPE) method<sup>[35,36]</sup> is a bottom-up technique for preparation of MOF thin films. It is a stepwise layer-by-layer growth process, which can be realized by alternatively emerging substrate into the inorganic component and organic linker solution. The unreacted or physical-adsorbed components are removed by rinsing with proper solvent between the deposition steps (Figure 2). Numerous

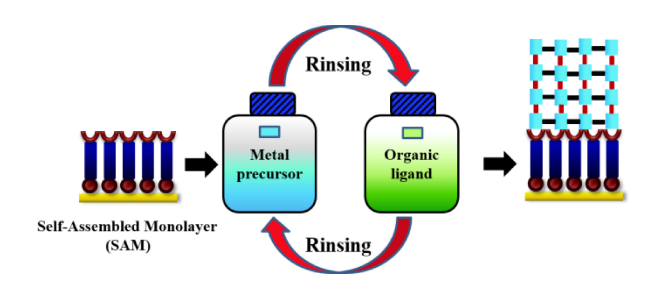


**Figure 2.** The stepwise layer-by-layer liquid-phase epitaxy approach for the growth of the thin film on SAM-functionalized substrate. The approach involves repeated cycles of immersion in solutions of the metal precursor and solutions of organic ligand.<sup>[35]</sup>

studies have well-documented details on how to prepare MOFs thin film using the stepwise LPE method. [37] So far, several new techniques of this method have been developed for MOF thin film preparation, namely pump, [38] spray, [39] dipping robot [40] and spin coating [41] methods.

Generally, functional SAMs with head groups of -OH, -COOH or pyridine on substrate are prepared. Similar to the in-situ growth approach, SAMs layer in LPE is not only beneficial to increase nucleation and growth but also very important for controlling MOFs orientation. The concentration of metal salt and ligand precursor solutions also needs to be noticed. Unlike most hydrothermal method, a relatively lower concentration of the precursor solution is necessary in the LPE approach because of better crystallization can be obtained in lower reagent concentration. Then the modified substrate is firstly immersed into the metal salt solution. The metal ions bind with head groups of the SAMs layer at the

surface and create the crucial first layer. In the next step, the substrate is washed with the solvent to eliminate the adsorption of excess salt (ethanol in most case). Then the substrate is put into the ligand solution for further reaction. After that, the substrate is washed again. By alternately repeating the above process, highly oriented and well-crystallized MOFs thin film with controllable thickness can be obtain. Apart from this dipping method, improved LPE approaches also have been developed. Instead of alternately dipping of the substrates into precursor solutions manually, the spray method is based on a system in which an aerosol is produced by expanding solutions of the reactants through a small nozzle of spray gun. This LPE approach can prepare MOFs thin film with a faster speed and keep a high degree of crystallinity and orientation. Additionally, oriented MOF films can also be prepared automatically by the LPE pump method in which the pump can control the precursor solutions into the reactor alternately. Notably, one of the merits of pump method better than the above two LPE methods is that it can perform thin film growth process under relatively higher temperature by circulating water/fluid system around the reactor.

LPE method has many obvious advantages: precisely controlled thickness, tunable growth direction, low roughness, high homogeneity and etc. Using this new method, the formation of interpenetrated networks can be suppressed because of the growth of layers of framework is constrained to a specific position on the underlying layer. [34] Even better, it can be possible to construct the MOFs thin films with crystalline order from the components of a material that is amorphous and very difficult to crystallize. [42,43] At present, most of the well-known crystalline-oriented thin films are fabricated by this method. A number of MOF films contain the SBU's like dimeric species (SBU: secondary building unit, [44] such as copper paddlewheel unit) or some containing more than one type of ligands have been developed by this method, such as [Cu<sub>2</sub>(ndc)<sub>2</sub>(dabco)]. [45,46,47] This method can be used to prepare the highly oriented thin film of MOFs with 2D layered structure, such as  $[M_2(bdc)_2(H_2O)_2]^{[48]}$  (M: Zn<sup>2+</sup>, Cu<sup>2+</sup>; bdc: benzdicarboxylate). It is noteworthy that this MOF-2-type structure thin film has not been obtained using conventional solvothermal conditions. The 3-D networked MOF thin films with controlled orientation can also be prepared by this method.  $[\{Zn_2((+)cam)_2(dabco)\}_n]$  ((+) cam: (1R,3S)-(+)-camphoric acid, dabco: 1,4-diazabicyclo (2.2.2)octane) thin film was fabricated by Liu and coworkers, [49] in which the growth direction of the thin film depend on the head groups of SAMs on the substrate. The [001] orientation was realized by pyridyl-terminated SAMs, and the [110] orientation was preferred when a COOHterminated SAMs was used. Another 3-D MOF Fe(pz)[Pt (CN)<sub>4</sub>] (pz: pyrazine) thin film with high crystallinity and orientation was fabricated by Otsubo et. al. in 2012.<sup>[50]</sup> The orientation of this film is highly controlled in both horizontal and vertical directions relative to the substrate. This report provides the first confirmation of details of not only the crystallinity but also the orientation of 3-D MOF thin film using synchrotron XRD.

To the best of our knowledge, the LPE technique is the most popular for fabrication of highly oriented MOF thin film. However, it still has a long way to go for the practical application. Firstly, the SAMs functionalized substrates are essential for the LPE approach, which limit the practical application of this method. In addition, it is highly time-consuming to fabricate MOF thin films by LPE method. It commonly needs at least half an hour or several hours to complete one-layer deposition. Although most of the MOF thin films fabricated in this method are under mild conditions, some MOFs with interesting properties can only be synthesized under very harsh condition, e.g. solvothermal reaction. Besides, most types of the MOF thin films fabricated by this method are SBUs-MOF, which show narrow range of application.

### 2.3. Layer-by-layer Method Coupled with the Langmuir-Blodgett (LB) Technique

As an excellent technique for the fabrication of monolayers on liquid substrate surfaces, the LB method is often used to prepare orderly nanofilms. Choosing this technique, highly crystalline-oriented MOF thin films might be produced. In 2010, Makiura<sup>[20]</sup> and coworkers firstly designed and realized a highly crystalline-oriented MOF thin film, NAFS-1, using the LB technique coupled with layer-by-layer (LB-LbL) method. Subsequently, a series of similar MOF thin films (NAFS-2, NAFS-13, NAFS-21, etc.)<sup>[51-55]</sup> were fabricated following the same method. Recently, R. Dong and his coworkers reported a two-dimensional MOF nanosheet made from THT and Ni (THT: 1,2,5,6,9,10- triphenylenehexathiol, 2DSP: two-dimensional supramolecular polymers) by LB method. [56] This is a free-standing single-layer sheet (0.7-0.9 nm in thickness) with large-area (square millimeters). After immobilized the THTNi 2DSP sheet on an electrode surface, an outstanding electrocatalytic performance in the hydrogen evolution reaction (HER) can be exhibited.

The general steps for the fabrication of MOF thin film by LB-LbL method are described here taking the example of NAFS-1 (Figure 3). In this method, the metalloporphyrin (CoTCPP) and a capping organic ligand (pyridine) are first spread onto an aqueous solution of metal salt (CuCl<sub>2</sub>·2H<sub>2</sub>O) to form MOF monolayers. In this process, the 2-D layered MOF sheets are formed on the solution surface. Then, the monolayers on air-water interface are compressed by the container's walls. Keeping a suitable surface pressure, the

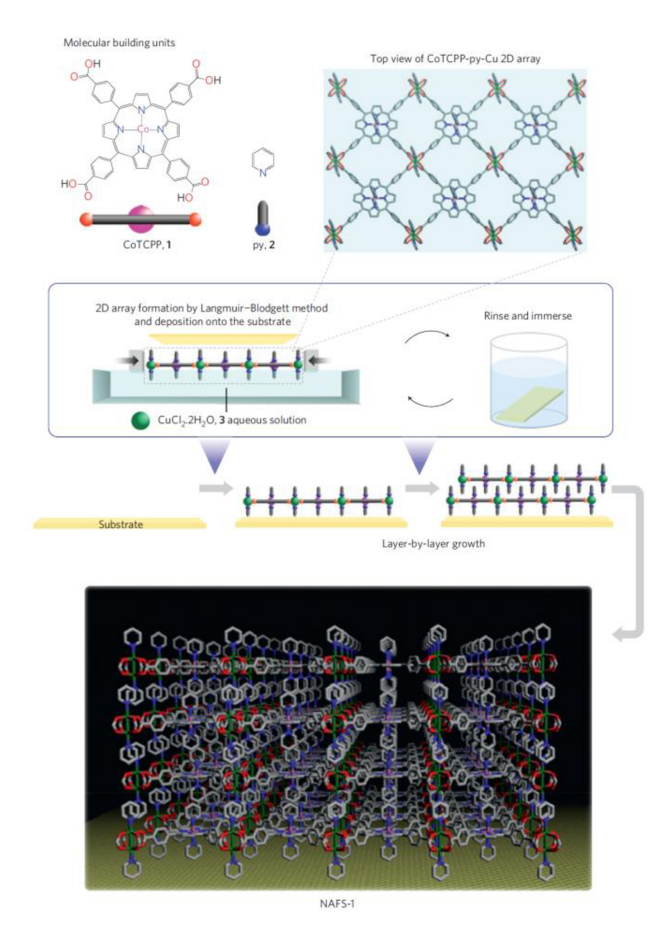


**Figure 3.** Schematic illustration of the fabrication method of NAFS-1. C atoms are shown in grey, N in blue, O in red, Co<sup>2+</sup> ions in pink and Cu<sup>2+</sup> ions in green. [20] Copyright 2010, Nature Publishing Group.

layered MOF sheets are transferred and stacked onto the substrate by following a LbL growth process. Because of the weak interactions ( $\pi$  stacking or Van der Waals interaction), the layers stack to interdigitated films (NAFS-1) after repeating several transfer cycles.

The MOFs thin films prepared by LB-LbL technology show low surface roughness and high homogeneity. The overall thickness of the film can be adjusted by the number of deposited layers and can be accurate to the nanometer level. It is worth to mention that variety of substrates can be used in this method and require no special treatment. Another significant advantage of this method is that the thickness of MOF film can be easily monitored by the UV-vis absorption spectrum. However, this method requires a LB film deposition device, which is quite expensive. The MOF film might be easy to fall off due to the weak interaction (Van der Waals' force) between the film and substrate. This method has the problem of small crystalline domain size at the initial period. [20] The NAFS-1 film shows domain size of ~ 20 nm. But later, Makiura<sup>[53]</sup> improved this method by using neutral

pyridyl groups as the peripheral porphyrin substituent to tune the metal-ligand interfacial coordinative reaction and prepared the NAFS-21 with sub-micron size (larger than 410 nm) in mono-molecular thickness. Recently, R. Dong also got a MOF single-layer sheet with large-area (square millimeters) using this method. [56] To date, this method has been only applied on 2-D layered MOF thin film system as its key step is the preparation of well-ordered 2D structure on the liquid surface. Moreover, this method was only reported performing under room temperature.

### 2.4. "Modular Assembly" Method

Utilizing normal laboratory instruments, the fast preparation of highly crystalline MOF thin films with high orientation is still a great challenge. In 2012, Xu and his coworkers reported a "modular assembly" approach to prepare MOF thin film, which is very powerful for fabricating oriented MOF thin films with large domain sizes.<sup>[21]</sup> Oriented MOF thin films can be prepared very simply in much less time than above mentioned thin film fabrication techniques. One of the best advantages of "Modular Assembly" protocol is that it separates thin film growth process into two steps, namely, "chemical synthesis" and "framework assembly". The "chemical synthesis" step allows people to produce highly crystalline "MOF modules" in all developed methods (including solvothermal method) for bulk MOFs synthesis. "MOF modules" normally with high-aspect-ratio are required, which can rapidly build MOF thin film through a simple "framework assembly" step.

The feasibility of "Modular Assembly" method is demonstrated by the successful preparation of CuTCPP thin film. As showed in Figure 4, Cu-TCPP nanosheets of with high-aspect-ratio are firstly synthesized by the solvothermal reaction of Cu(NO<sub>3</sub>)<sub>2</sub> and H<sub>2</sub>TCPP (5,10,15,20-tetrakis(4-carboxyphenyl) porphyrin). Then, the flaky MOF nanosheets are dispersed in ethanol to form a purple colloidal suspension. After that, the suspension is dripped drop-wise onto the surface of water in a beaker. At this step, the Cu-TCPP nanosheets fan out to be a thin film spontaneously because of the hydrophobic property of the nanosheets. Finally, the thin film can be easily transferred to a solid substrate via a "stamp" process, and the thickness of the thin film can be controlled by repeating the stamping assembly process.

This "Modular Assembly" approach connects the research of nanomaterial and MOF thin film preparation which may overcome the weakness of the traditional method, and possesses a lot of gigantic advantages. For example, solvothermal reaction can be coupled into MOF thin film preparation. This method enables to rapidly build MOF thin film through a straightforward way. A highly oriented quasi-single crystalline MOF thin film of 100 layers can be prepared within 10

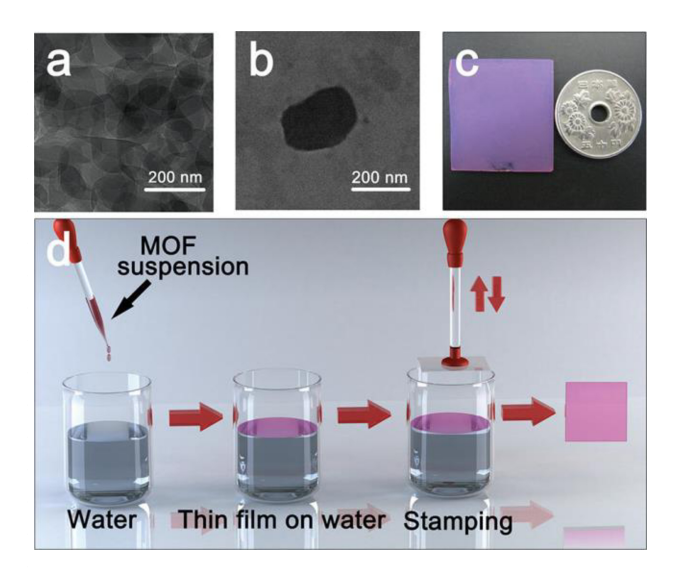


**Figure 4.** (a, b) TEM images of the synthesized Cu-TCPP nanosheets. (c) Photograph of the MOF thin film after 15 deposition cycles on a quartz substrate. (d) Illustration of the assembly process of this MOF thin film. [21] Copyright 2012, American Chemical Society.

minutes, while it may need more than a dozen hours in other methods. The MOF thin films fabricated by this method hold many nice traits, such as crystalline state, oriented framework, controlled growth, and ultrathin in thickness. However, there are still numerous obstacles hampering the realistic application of "Modular Assembly" on MOF thin film preparation. Theoretically, "Modular Assembly" could be applied to MOFs with all kinds of crystal structure, as long as MOFs could be prepared with high-aspect-ratio flaky nanostructure. MOFs thin films with 2D framework structure could be possibly controlled to form flaky nanostructure. However, it is a challenge to prepare the MOFs nano-sheet with 3D structure. Moreover, the orientation of MOF thin film made by "Modular Assembly" depends on the orientation of the nanosheets prepared by chemical synthesis. It needs to develop a synthetic method to prepare MOF nanosheets with different crystallographic orientation to achieve the fabrication of MOF thin film with different orientations. For practical applications, to increase the freedom of controlling different orientation of the MOF thin film is required.

### 3. The Applications of Crystalline, Highly Oriented MOF Films

Numerous physical and chemical properties have been investigated in the literature for a wide range of applications based on MOF films, and some reviews have also been

published. [14,57,58] In some specific applications, such as gaspermeable and separation, the MOF thin films with predetermined thickness and well-defined orientation are essential. [59] However, the use of crystalline, highly oriented MOF films for different applications is still in a nascent yet promising stage. Thus, it is crucial for practical applications to investigate the fundamental properties of oriented MOF thin film. Highly oriented crystalline MOF thin films have been tentatively applied in the following five fields: (1) Optical applications, (2) Adsorption/Separation, (3) Enantioselective, (4) Template system, and (5) Electrical applications.

### 3.1. Optical Applications

The MOF films with different kinds of optical properties (color, refractive index, luminescence, photochromism, photosensitivity, etc) show potential applications in the devices. Among the works of optical applications based on MOF films in recent years, [60-67] oriented MOF films with luminescence, photoswitching and other properties have drawn significant attention. In this section, we review the current literatures in which the oriented MOF films serve as active components for the optical properties.

High quality MOF thin films often exhibit excellent optical properties. Redel et. al. [63] fabricated two highly porous, crystalline MOF thin films, HKUST-1 and Cu-BDC (benzenedicarboxylate), on modified silicon substrates using LPE method. The produced MOF thin films are smooth and crack-free. It can be seen the homogenous interference color over the entire sample. Therefore, it is greatly simplified to determine the optical constants, such as refractive index of these two SURMOFs (surface-attached crystalline and oriented metal-organic framework multilayers) by using spectroscopic ellipsometry (SE), which is very difficult to determine for the standard powder of these porous solids. Gu et.al<sup>[40]</sup> found that high quality HKUST-1 films with welldefined thickness and orientation also showed tremendously improved transparency. The MOF film prepared with ultrasonication is significantly clean, homogenous and has a considerably small surface roughness. The optical transmission spectra showed that the sample is basically transparent in the visible range and absorbs light only for wavelengths below 350 nm.

For the luminescence MOF thin films based on the implanted dye guest species into the pores of MOFs, the oriented MOF thin films often show better optical property than the anisotropic films. Streit et. al. [67] prepared a 3D porous MOF (HKUST-1) thin film with an inorganic dye as guest species [Eu(bzac)<sub>3</sub>bipy] (bzac = l-phenyl-1,3-butanedionate, bipy = bipyridine) inside the MOF pores (Figure 5). By immersing the MOF films fabricated by LPE method into the ethanolic solutions with luminescent molecules, a high

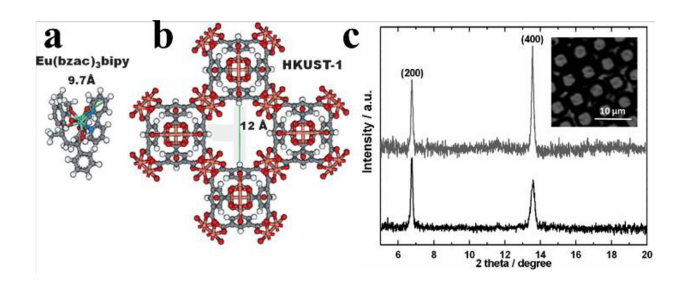


**Figure 5.** (a) Size of the Eu(bzac)<sub>3</sub>bipy complexes and (b) the pore size estimation of HKUST-1. (c) XRD diffract gram of HKUST-1 SURMOF before (black curve) and after (gray curve) loading with Eu(bzac)<sub>3</sub>bipy. Inset: fluorescence image of laterally patterned HKUST-1 SURMOF sample loaded with Eu(bzac)<sub>3</sub>bipy and irradiated by UV light at  $\lambda = 366$  nm. The bright features represent the SURMOF structures, loaded with the Eu<sup>3+</sup> complex. [67]

filling factor could be achieved. Because of the high orientation in the high-quality MOFs thin films, 30% of the pore can be loaded with the luminescent compound, which is much higher than the powder materials fabricated by conventional solvothermal methods. The spectra measurements reveal an effective energy transfer between the HKUST-1 and the Eu<sup>3+</sup> ion, which is determined by the match of donating levels of the sensitizers (here the btc-ligands within the HKUST-1 framework) and the accepting energy levels. The MOF works effectively as an antenna to convert incident radiation into electronic excitations and then transfer them to the Eu<sup>3+</sup> ions. It can be anticipated that much more efficient systems based on the oriented MOFs thin films may become available in the near future.

An attractive alternative to incorporate MOFs into a solar energy conversion device is to fabricate MOFs thin films with precise optimization of optical path length and crystal-thickness. With this in mind, So and coworkers had successfully prepared luminescent, chromophore aligned, porphyrinic MOF films (Figure 6). [68] Using an automated

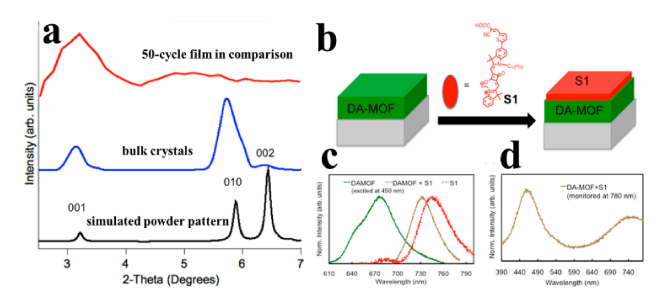


**Figure 6.** (a) X-ray reflectivity scans of the DA-MOF. (b) Schematic diagram of preparation of sensitized DAMOF film. (c) Comparison of emission profiles of DA-MOF (green solid), S1 (red solid), and DA-MOF sensitized with S1 (light-green dotted) upon excitation at 450 nm. (d) Excitation profile of the DAMOF+S1 film monitored at 780 nm, where the emission from DAMOF is negligible. [68] Copyright 2013, American Chemical Society.

LbL assembly technique, the porphyrin-based MOFs thin films with porosity, controlled thickness and orientation were fabricated. In these films, porphyrin building blocks are preferentially aligned. By installing a supplementary chromophore, a far-red emitting squarine dye (S1), atop the outermost layer of investigated 50-cycle film (Figure 6b), efficient long-distance migration between aligned assembled porphyrins and ultimately trapping to S1 indeed occur within the MOF film. This finding indicates that the porphyrin-based MOF films with highly orientation have the potential utility for light-harvesting and efficient energy transport in solar energy conversion devices.

Liu and coworkers had performed a good attempt to introduce luminescent molecules onto oriented MOFs films for tuning the optical properties. They demonstrated the first example of layer-selective installation of functional groups at the external surface of MOF thin film, which displays expected luminous property. [69] By means of LBL-LPE, the [001]-oriented [Cu(ndc)(dabco)<sub>0.5</sub>] (ndc = 1,4-naphthalene dicarboxylate, dabco = 1,4-diazabicyclo[2.2.2]octane) thin film was fabricated. With the ligand exchange between acetate and 2-amino-1,4-benzeneterephtalate (NH2-bdc), the amino functionalized SURMOF could be deposited, which was changed from inert [Cu(ndc)(dabco)<sub>0.5</sub>] film to an active material. Then, covalent fluorescein isothiocyanates (FITC) were bonded at the external surface of MOF thin film by the reaction between NH2 groups of MOF thin film with isothiocyano group of luminescent molecule. Consequently, a significant increased fluorescence intensity is observed in fluorescence microscopy images (Figure 7). This method offers unique possibility for investigation of MOF chemistry that cannot be accessed by conventional one-pot solvothermal reactions. In this example, MOFs thin films are deposited in selected orientations with well-defined terminal compositions. That is the key to ensure the post-synthetic modification (PSM) occur at the external surface of the MOF multilayer film. This SURMOF-based concept can be proposed to further investigate and develop the MOF surface, interface, and host-guest chemistry in general.

The remote control of surface properties can be realized by oriented MOF thin films equipped with photoswitchable linkers. Utilizing a highly oriented SURMOF-based hybrid film system, Heinke and coworkers reported a two-component hybrid system which can be switched by light. This smart film system was fabricated by the LPE method and the combinations of vertical compositional gradients with the same orientation had been realized. The structure of this system is shown in Figure 8. The basic layer of Cu<sub>2</sub>(BPDC)<sub>2</sub> (BiPy) (BPDC: biphenyl-4,4'-dicarboxylic acid, BiPy: 4,4'-bipyridine) grows essentially in the [001] direction. Then, a second layer of Cu<sub>2</sub>(AB-BPDC)<sub>2</sub>(BiPy) (AB-BPDC: 2-azobenzene 4,4'-biphenyldicarboxylic acid) is deposited with

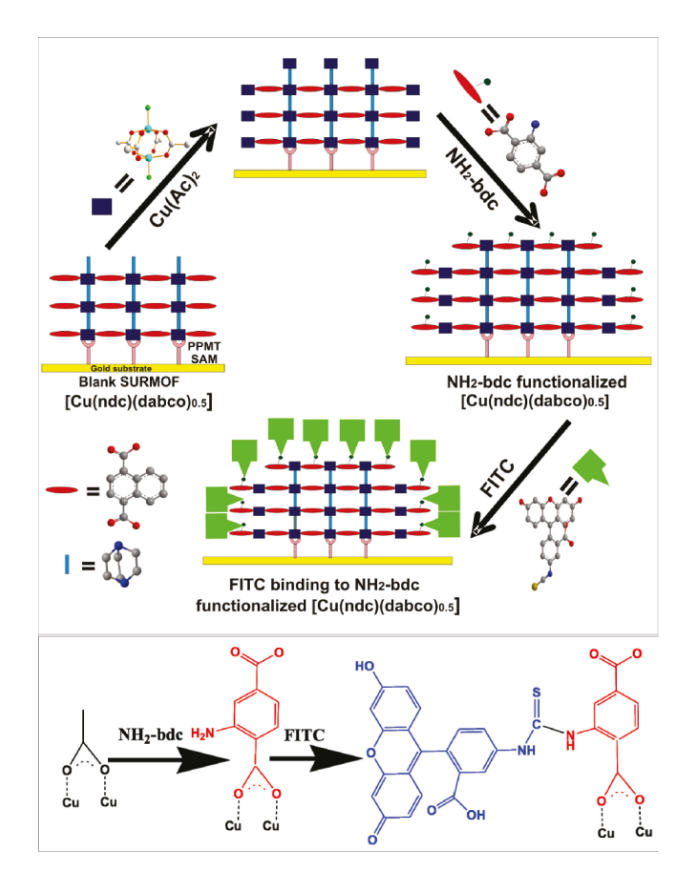


**Figure 7.** Stepwise approach for external surface functionalization of the preformed [001]-oriented SURMOF. [Cu(ndc)(dabco)<sub>0.5</sub>] at pyridine-terminated PPMT SAMs and (bottom) ligand exchange between acetate and NH<sub>2</sub>-bdc and reaction of NH<sub>2</sub>-bdc with FITC. <sup>[69]</sup> Copyright 2011, American Chemical Society.

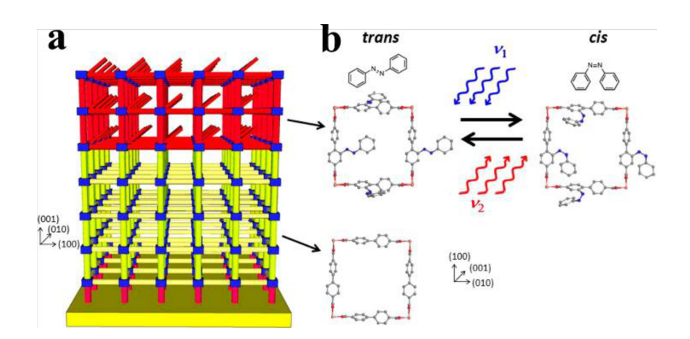


**Figure 8.** Sketch of the layered photoswitchable SURMOF. (a) The bottom, passive SURMOF is grown on the gold substrate, and an active SURMOF containing photoswitchable azobenzene is grown on top. (b) View of the pore window in the [001] direction. The azobenzene embedded in the MOFs structure as well as molecular azobenzene can be switched from the trans to the cis state by UV light (v1) and vice versa by visible light (v2). [70] Copyright 2014, American Chemical Society.

the same orientation. The bottom layer, which contains 1.5 nm pores, can store guest molecules and serves as a reservoir. The top MOF layer contains a photo-switchable

azobenzene-based strut, which is an active part of the hetero-SURMOF. This layer can be switched from trans to cis form by irradiated with ultraviolet light. It is responsible for the optically induced uptake and release of guest molecules. This hybrid SURMOFs system allows a straightforward realization of functional coatings with optical remote control. This approach has potential to realize photon-driven pumps and other photon energies devices.

Another typical example is the chemical sensor based on the optical and luminescent properties of MOF film. Lu and coworkers<sup>[71]</sup> had prepared a ZIF-8 film based Fabry-Pérot sensor by the process of alternately immersing the glass slide into the precursor solutions containing zinc nitrate and 2-methylimidazole (Figure 9). The obtained ZIF-8 films show

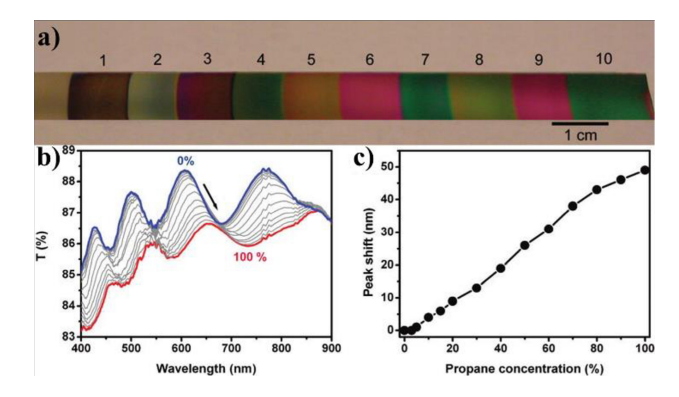


**Figure 9.** (a) Photograph of a series of ZIF-8 films of various thicknesses grown on silicon substrates. (b) UV-vis transmission spectra of 10-cycle ZIF-8 film grown on glass substrate after exposure to propane of various concentrations (blue curve for 0 % and red curve for 100 %) and (c) corresponding interference peak (originally at 612 nm) shift versus propane concentration. [71] Copyright 2010, American Chemical Society.

relatively good orientation in [001] direction. Moreover, these films with various thicknesses show variable coloration which was a manifestation of film-thickness-dependent optical interference in the visible region. Because of the resonating properties of interferometer and the absorption feature of porous ZIF-8, different transmission spectra can be obtained by exposing the film to various vapours. Therefore, this ZIF-8 based Fabry–Pérot device can distinguish between linear hexane and bulky cyclohexane. The ethanols in water as low as 0.3 % v/v can also be detected which corresponding to an ethanol concentration of 100 ppm. As a selective sensor for chemical vapors and gases, this device shows immense potential applications beyond chemical/biomedical devices, including medical detection.

### 3.2. Selective Adsorption/Separation

As anisotropic crystallographic systems, MOFs often exhibit obvious different adsorption kinetics for adsorbents approaching at different directions owing to varied pore openings and channels. Therefore, the well-oriented MOF thin films/membranes (membrane most commonly means a thin, selective barrier, but it is sometimes used for films that function as separators, like biological membranes.) can provide an alternative way to explore the adsorption/separation properties in different orientation. [34,72–80]

Allendorf et. al.<sup>[72]</sup> firstly fabricated a mechanochemical sensor based on HKUST-1 film which was grown on a gold-coated, SAMs functionalized microcantilever surface using the LbL method (Figure 10). The device for this investigation

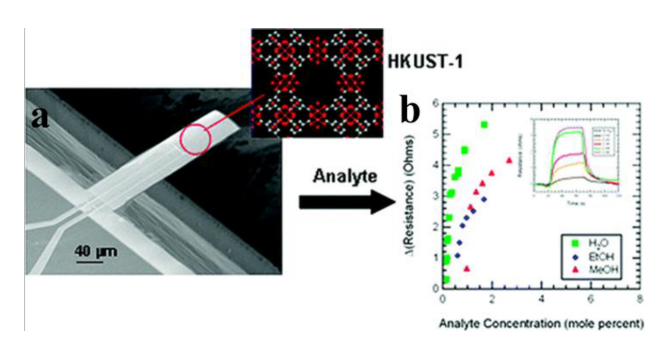


**Figure 10.** (a) The SEM image of piezoresistive microcantilever (the inset is the crystal structure), (b) Resistance change versus analyte concentration expressed as a percentage of the total gas flow (balance N<sub>2</sub>) at 298 K and 1 atm. (the inset: temporal response of the cantilever piezoresistive sensor to water vapor diluted in N<sub>2</sub>). <sup>[72]</sup> Copyright 2008, American Chemical Society.

was a 10-microcantilever array, in which each cantilever incorporated a built-in piezoresistive sensor for stress-based detection. This sensor was weakly responsive to the small gaseous guest molecules, but rapid and reversible responsive to H<sub>2</sub>O, MeOH and EtOH. The HKUST-1 in dehydrated state was reported respond to CO<sub>2</sub>, which was further extended to the detect of VOCs. <sup>[73]</sup> This piezoresistive microcantilevers were able to detect 12 different VOCs and distinguish among them based on the difference of the shape, response time and signal amplitude. This device showed great potential applications in breath analysis and gases detection.

Liu and coworkers demonstrated the orientation-dependent adsorption behaviors of volatile organic compounds by using the crystallized [Cu<sub>2</sub>(ndc)<sub>2</sub>(dabco)] thin films in the [100] and [001] orientations, respectively.<sup>[74]</sup> These films were fabricated individually on pyridyl- and carboxylate-terminated SAMs substrates by LPE method to control their pore opening at the [001] and [100] direction (Figure 11).

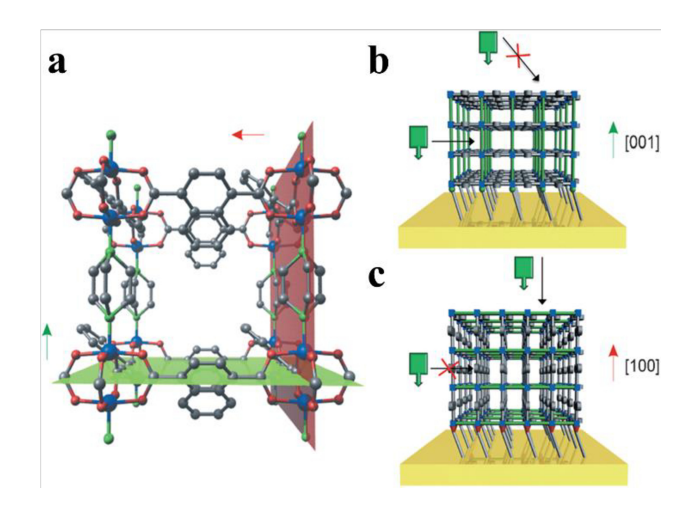


**Figure 11.** (a) Crystallographic structure of  $[Cu_2(ndc)_2(dabco)]$ , showing the [100] and [001] direction. Schematic illustration of a  $[Cu_2(ndc)_2-(dabco)]$  thin film fabricated on a PPMT (b) and MHDA (c) SAMs having a [001] and [100] orientation, respectively. Their orientation dependent adsorption behaviors are also depicted. [74]

These two MOF thin films in [100] and [001] orientation were allowed to investigate the orientation-dependent adsorption behaviors by utilizing quartz crystal microbalance (QCM) against mass change (Figure 11). As expected, even though their components and structures are identical, different behaviours in the (kinetic) adsorption selectivity of benzene, toluene, and xylene were observed. The thin film with orientation in the [100] direction shows a larger pore opening perpendicular to the exposed substrate favored a faster guest molecule uptake and thus leads to a higher (kinetic) adsorption selectivity. This results demonstrate that the orientation and stacking of MOF thin films play significant roles in the adsorption properties by controlling guest access to the pores in MOFs. Based on this work, the investigations of the controllable adsorption/permeation rate in MOFs thin films/membranes can be achieved by adjusting orientations and morphologies.

Another typical example of orientation-dependent adsorption behaviors is heterostructured MOF films system. Fischer and Kitagawa had reported several heterostructured SUR-MOFs with different properties, for instance, selectivity, storage capacity and hybrid adsorption. [75–78] All of the adsorption properties of the heterostructured SURMOF systems are statistically relative to the orientation of thin films. In addition, certain properties (such as preferential adsorption in mixed gas, [75] hybrid adsorption properties [77]) are also demonstrated by extra changes in the heterostructured systems. Taking the heterostructured SURMOFs system of [Cu<sub>2</sub>(NH<sub>2</sub>-bdc)<sub>2</sub>(dabco)] (**A**) on top of [Cu<sub>2</sub>(bdc)<sub>2</sub>(dabco)] (**B**) as an example, [75] Tu and coworkers fabricated this heterostructured SURMOFs on pyridyl-terminated Au cov-

ered QCM substrate using a LPE growth approach. The orientation of this SURMOF **B@A** is [001] direction on Au surface which was confirmed by the XRD. By way of PSM using *tert*-butyl isothiocyanate (*t*-BITC), the pore size of the top layer [Cu<sub>2</sub>(NH<sub>2</sub>-bdc)<sub>2</sub>(dabco)] (**B**) becomes smaller. This SURMOF **B@A** with integration of two spatially separated functions exhibits size selectivity owing to the small pore size of the top layer and the high storage capacity of the bottom layer.

The spatial arrangement of each component in the hetero-MOF films also influences the adsorption behaviors. Meilikhov et. al. [76] prepared three binary "Janus MOF" composed of tetragonal pillared-type MOFs:  $\mathbf{A} = [Cu_2(ndc)_2 (dabco)]_n$  and  $\mathbf{B} = [Cu_2(NH_2\text{-bdc})_2(dabco)]_n$ . Framework  $\mathbf{B}$  can be further modified with succinic acid anhydride to form  $\mathbf{C} = Cu_2(HOOC(CH_2)_2OCNH\text{-bdc})(NH_2\text{-bdc})(dabco)]_n$  (Figure 12). Type  $\mathbf{I}(\mathbf{C@A})$  and Type  $\mathbf{II}(\mathbf{A@C})$  thin films are

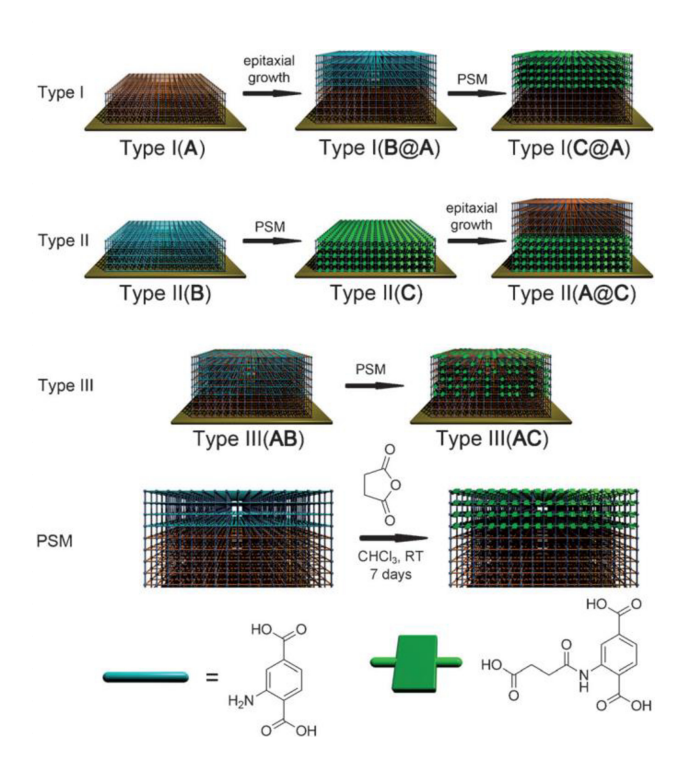


**Figure 12.** Different types of heterostructured Janus MOF coatings with MOF frameworks A:  $[Cu_2(ndc)_2(dabco)]_n$ ; B:  $[Cu_2(NH_2-bdc)_2(dabco)]_n$ ; C:  $[Cu_2(HOOC(CH_2)_2OCNH-bdc)_2(dabco)]_n$  and the principle of postsynthetic modification of Janus MOF coatings exemplarily demonstrated for Type I(B@A) material. [76]

preferentially oriented in the [001] direction and exhibit the same chemical composition. However, two different spatial configurations (face-up or face-down configuration) are displayed. Whereas Type **III(AC)** thin film is homogeneous MOF system without spatial separation. By adsorption test of

single and multiple volatile organic vapors, it can be found that the change of spatial arrangement of **A** and **C** can influence the directional permeability and selective adsorption behavior. Type **I**(**C**@**A**) thin film can selectively adsorb small and polar VOC, methanol. However, the inversed structure of Type **II**(**A**@**C**) has no selectivity. Analogous results are obtained by mixture sorption experiments with Type **III**(**A**C) materials. Thus, the spatial arrangement in hetero-MOF thin films is of great importance to the adsorption properties. This heterogeneous hybridization concept can be implemented in device coatings for the precise tuning of sensing performance and in the field of electronics with higher chemical complexity.

Very recently, H. Kitagawa and co-workers had described the new sorption properties in a series of Hofmann-type crystalline oriented MOF thin films. These thin films were fabricated by LPE method and showed highly oriented crystalline nature and remarkable lattice shrinkage. The typical example is the 2D interdigitated thin film of {Fe (py)<sub>2</sub>[Pt(CN)<sub>4</sub>]} (py, pyridine) which showed dynamic guest-sorption behaviour (Figure 13). This guest uptake with a

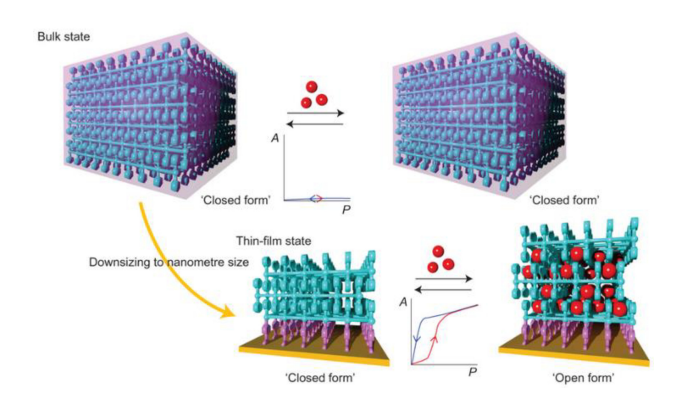


**Figure 13.** Schematic representation of the structural responses in the coordination frameworks. Dynamic structural response to guests induced by crystal downsizing from the bulk state to the nanometre-sized thin film for  $\{\text{Fe}(\text{py})_2[\text{Pt}(\text{CN})_4]\}$ . In this case, the bulk material shows no significant guest uptake, whereas in a thin film, a dynamic gate-opening response to the guest is observed. [83] Copyright 2016, Nature Publishing Group.

structural transformation behaviour is markedly suppressed with the increase of film thickness, and the bulk state of the same MOF showed no significant guest uptake. The in situ XRD, quartz crystal microbalance measurements and AFM-image indicated that this crystal-downsizing effect might be caused by the  $\pi$ - $\pi$  stacking between pyridine ligands in MOF, which prevented the guest penetration within the framework (or limited to the surface area) in the bulk state, and hindered the diffusion of guests in the thicker thin films. However, the effects of ligand  $\pi$ - $\pi$  interaction were decreased due to the reduced number of ligands at the outermost

surface in the thin-film state, that would contribute to the lowering of the potential barrier height for a gate-opening-type guest uptake. In addition, this film also exhibited selective guest uptake accompanied by anisotropic expansion along the vertical direction to the substrate surface. These findings have the potential for the functional applications, such as chemoswitching or sensing applications, catalytic devices and integrated systems of functionality.

The MOF with tunability of pore size and sorption behavior makes it an ideal candidate as membrane for gas separation. [84] In the past five years, the MOF membranes/films of ZIF-8, [85] ZIF-69, [86] ZIF-90, [87] HKUST-1 [88,89] have been studied carefully as separators and sensors. These materials present good performance in separation, such as CO<sub>2</sub> adsorption-driven selectivity separation, [90] H<sub>2</sub>/CO<sub>2</sub> separation, [91] even organic solvent nanofiltration. [92] Herein, we select the typical examples of MOF membranes to show the influence of different orientation of MOFs in the separation property.

Li and coworkers prepared a ZIF-7 membrane with preferred c-out-of-plane orientation (Figure 14) by dip-coat-

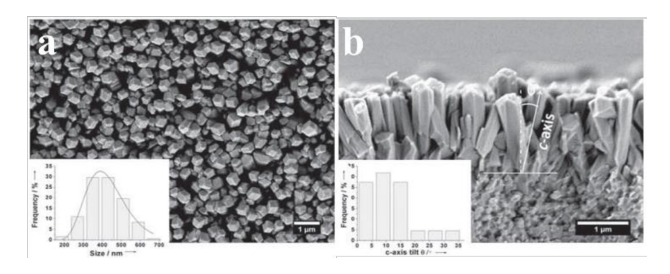


**Figure 14.** SEM top views and cross sections of the ZIF-7 membranes obtained after 225 min of microwave assisted secondary growth. Insets in the SEM top views give the distributions of the cross-sectional size of the columnar crystals, and the CPO distributions. The CPO is represented by the angle y between the c axis and the substrate normal. [93]

ing and microwave assisted secondary growth process. [93] This oblique crystallographic preferred orientation (CPO) cannot be simply described as 101 CPO, but can be well explained by refined evolutionary selection in a vander Drift-type growth. [94] This ZIF-7 membrane was chosen to evaluate the gas separation property by the test of equimolar H<sub>2</sub>-CO<sub>2</sub> gas mixture. Compared with the randomly oriented ZIF-7 membrane, [95] the oriented ZIF-7 membrane exhibits an increase in selectivity with temperature. The H<sub>2</sub>-CO<sub>2</sub> mixture separation factor of 8.4 was measured at 200 °C, which is much larger than the Knudsen separation factor of 4.7. However, the H<sub>2</sub> permeance of the oriented membrane is one-tenth that of the randomly oriented membrane. The probable reason may be ascribed to the anisotropic pore structure of ZIF-7 crystals, both the pyramidal termination

[101] faces and the prismatic [110] faces of the crystals possess direct entrances for guest molecules. This result shows that manipulation of the channel orientation and grain morphology of the MOF films is of great significance for the applications of MOF thin films in related advanced nanodevices.

Subsequently, Bux and coworkers demonstrated a highly oriented ZIF-8 composite film on top of a porous alumina support, which the film showed preferred orientation with [100] plane parallel on the supports (Figure 15). [96] In gas

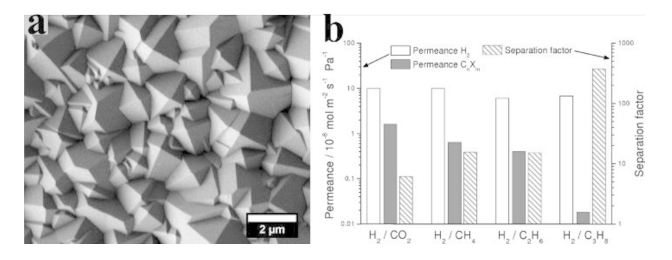


**Figure 15.** (a) SEM top view of the well-intergrown ZIF-8 layer after 2 h of secondary growth. (b) Permeances and separation factors (in logarithmic scale) of equimolar  $H_2/C_nX_m$  gas mixtures at room temperature measured on the ZIF-8 membrane prepared by 2 h of secondary growth. [96] Copyright 2011, American Chemical Society.

mixture permeation experiments, this orientation membrane showed good performance in H<sub>2</sub>/hydrocarbon separation. With respect to the H<sub>2</sub>/CH<sub>4</sub> separation factor, the oriented ZIF-8 membrane with the improved quality of the microstructure showed a slightly higher selectivity in comparison to non-oriented film.<sup>[97]</sup> The author explained that owing to the cubic symmetry of the 3-D pore network of ZIF-8, the crystal orientation is expected to have minor influence on membrane permeation and the separation performance on the macroscopic level.

### 3.3. Enantioselective

Liu and coworkers<sup>[49]</sup> demonstrated the first example of enantioselective adsorption on SURMOF  $[Zn_2(+/-) cam_2 dabco]_n$  (cam = camphoric acid, dabco = 1,4-diazabicy-clo(2.2.2)octane) in 2012 (Figure 16). The enantiopure MOF thin films with the orientation of [110] and [001] on MHDA and PPMT SAMs were prepared. The adsorption kinetics of the enantiomeric SURMOFs can be monitored and characterized by using QCM device. In the systems of  $[Zn_2+cam_2 dabco]_n$  and  $[Zn_2-cam_2 dabco]_n$  with [110] orientation, the adsorption test of (2R,5R)-2,5-hexanediol (R-HDO) and (2S,5S)-2,5-hexanediol (S-HDO) showed different absolute uptake and absorption rate, which indicated significant enantioselectivity. However, QCM cannot distinguish R- from S-HDO by the mass uptake only, thus, the

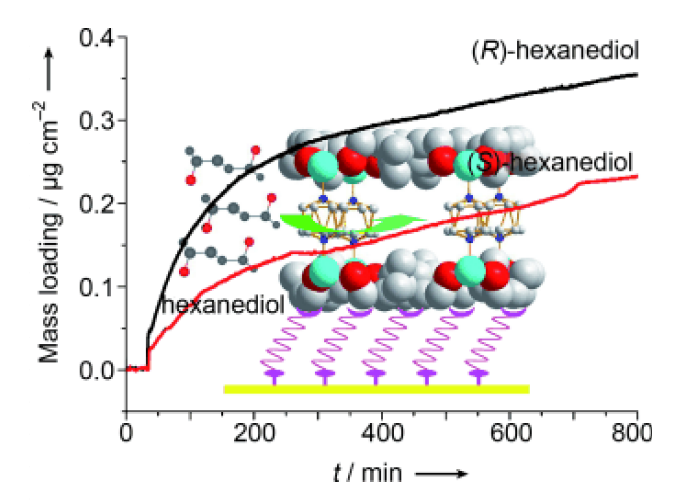


**Figure 16.** Schematic illustrations of oriented MOF film on gold substrates and the QCM profiles of specific mass uptake of each enantiomer from the gas phase: *R*-HDO (black) and *S*-HDO (red) over (+)-1 (20 cycles). [49]

data on racemate separation cannot be gained. The results may serve as valuable devices for (high throughput) automatic screening MOFs and analytes to optimize enantioselectivity in chiral separations.

Oriented circular dichroism (OCD) was selected to characterize the ratio of two enantiomers loaded into homochiral SURMOF. Gu and coworkers [98] carried out this study in 2014 for the first time. Three-dimensional chiral SURMOFs with the composition of  $[Cu_2-(Dcam)_{2x}(Lcam)_{2-2x}(dabco)]_n$  (dabco = 1,4-diazabicyclo-[2.2.2]- octane) were fabricated on quartz glass by layer-by-layer LPE method (Figure 17). The growth direction can be switched between [001]

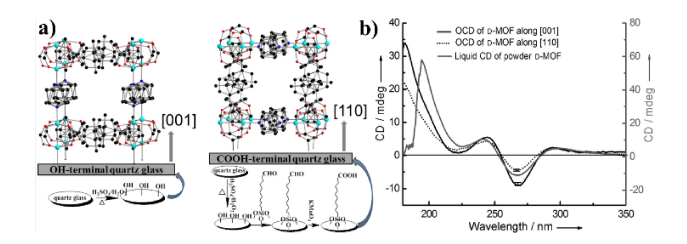


**Figure 17.** (a) Structures of the  $[Cu_2(Dcam)_2(dabco)]_n$  SURMOF grown in the [001] and [110] directions. (b) OCD spectra of d-MOF grown in the two perpendicular orientations [001] and [110] (left y axis) and conventional CD spectrum of a suspension of the corresponding MOF powder (right y axis). <sup>[98]</sup>

and [110] directions by using OH- and COOH-terminated substrates. The orientation of the enantiomeric linker molecules was confirmed by the OCD. As expected, the  $[Cu_2(Dcam)_2(dabco)]_n$  grown in [001] and [110] directions showed different OCD band intensity (Figure 17b). This was due to the anisotropic nature of the chiral SURMOFs, which

was further confirmed by theoretical calculation. The enantiopure  $[Cu_2(Dcam)_2(dabco)]_n$  and  $[Cu_2(Lcam)_2(dabco)]_n$  SURMOFs were used to explore selective enrichment upon loading from the racemic mixture of chiral ethyl lactate [(+)-ethyl-d-lactate and (-)-ethyl-l-lactate)]. Enantioselective enrichment of >60% was observed when the chiral host scaffold was loaded with the racemic mixture. This investigation shows valuable potential application in filter and membrane materials, which can contribute to the highly topical field of enantiomer separation.

Soon after, Gu and coworkers<sup>[99]</sup> further studied the influences of pore size of homochiral SURMOF on enantioselective adsorption. Three isoreticular chiral SUR-MOFs  $Cu_2(Dcam)_2(L)$  (Dcam = (1R,3S)-(+)-camphoric acid) with [001] growth orientation and high crystallinity were prepared. These SURMOFs showed identical stereogenic centers but different pore dimensions. The enantioselective uptake of SURMOFs to the chiral probe molecules ((R)- and (S)-limonene) has been studied by using QCM device. Although the adsorption capacity increased with the increase of pore size, the enantiomer selectivity exhibited more complex situation. The highest enantiomeric excess was observed at the medium pore size (0.8 nm in Cu<sub>2</sub>(Dcam)<sub>2</sub> (BiPy)), while the enantiomeric excess in very small or large pore was significantly smaller. This study demonstrates that both the stereogenic center and the suitable pore size are important parameters for chiral nanoporous materials to gain higher enantioselectivity.

#### 3.4. Template System

Utilizing MOF as template, three-dimensional (3D) materials with high porosity and well-defined structure can be fabricated. Tsotsalas and coworkers [100] fabricated a 3D, highly porous, covalently bound polymer film with homogeneous thickness by using an oriented SURMOF (Figure 18). Through the conversion process of ligands covalently crosslink with each other in SURMOF, the hierarchically structured gels with vertical composition gradients were established. Subsequently, the metal-free, water-stable coatings (called surface-mounted gels, SURGELs) were produced in the form of well-defined oriented layers after the metal ions in SURMOF were removed. This SURGEL combine the advantages of MOF and gel materials. It offers great variability for introducing functional groups into framework and show high flexibility and large pore size in the structures. Additionally, the SURGELs is a robust framework comprising of covalent bonds and pronounce stability under biological condition.

This novel method to fabricate SURGELs represents a versatile strategy for creating laterally and vertically structured thin films of gel materials, which own tailorable properties

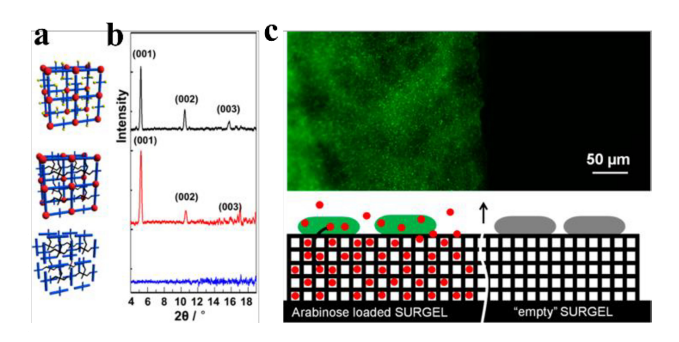


**Figure 18.** (a) Schematic representation of the cross-linking process within the SURMOF-2 structure before the cross-linking reaction (top), after the cross-linking (middle), and after treatment with EDTA for 30 min (bottom). (b) Corresponding X-ray diffraction (XRD) data. (c) Schematic representation and fluorescence microscopy images of P. putida pJN::GFP bacteria after 24 h of incubation in the presence of URGEL substrates. Top: bacteria settled on the SURGEL substrate containing arabinose. Bottom: bacteria settled on an "empty" SURGEL substrate. [100] Copyright 2014, American Chemical Society.

and show a huge potential application. Tsotsalas and coworkers88 demonstrated the possibility of loading SURGELs with bioactive compounds (Figure 18 c). By loading arabinose (as a prototype biomolecule) into the SURGEL, the substrate was exposed to bacterial cells genemodified with an arabinose-triggered GFP switch. Arabinose will induce GFP expression in these microbes in a highly selective manner. The bacterial cells adhering on the surface of arabinose-loaded SURGEL showed GFP fluorescence. In contrast, bacterial cells adhered on SURGEL surfaces without previously loaded arabinose showed only marginal GFP fluorescence. The results indicate that the SURGELs can be implemented as bioactive coatings and provide a drug-release platform in vitro cell culture studies.

The SURGELs can also offer a robust platform for the attachment of functional moieties. Mugnaini et. al. [101] successfully incorporated ferrocenyl thiol derivative (6-(ferrocenyl)-hexanethiol) into the SURGELs by using thiol-yne click reaction. This ferrocene modified SURGEL showed much higher currents and larger separations of the oxidation/reduction peaks compared to insulate SURGEL, in cyclic voltammetry (CV). It is fully compatible with Nernstian diffusion of the redox species within the modified SURGELs. This finding opens the door to use SURGELs for electrical applications.

### 3.5. Conducting Properties

An appealing approach toward the development of more efficient and robust electronic devices is tuning the electrical properties of thin films by controlling technologies. Dragässer et. al. [102] improved the electro-chemical properties of highly ordered, crystalline HKUST-1 film by using ferrocene as an

immobilized redox mediator. The ferrocene, which was loaded by vapor phase method, acted as redox-mediators to establish charge transport across the insulating HKUST-1 film. As a suitable inner-sphere redox system, the ferrocene@-Cu<sub>3</sub>(BTC)<sub>2</sub> film showed good charge transport properties and a large increase in conductivity as high as  $\sim 10^{-9}~\rm S~cm^{-1}$ , exceeding that of HKUST-1 film by several orders of magnitude. These results show that high quality doped thin MOF films have excellent potential for electrochemical and electronic applications.

An alternative strategy to modulate electrical conductivity of MOFs was recently attempted by Talin et. al. [103] The guest molecules [7,7,8,8-tetracyanoquinododimethane (TCNQ)] were introduced into the pores of Cu<sub>3</sub>(BTC)<sub>2</sub> thin films by immersing the HKUST-1 films into saturated TCNQ/ CH<sub>2</sub>Cl<sub>2</sub> solution. The conductivity of HKUST-1@TCNQ increased nearly six orders of magnitude. Supported by structural, spectroscopic, and modeling analysis, the author demonstrated that the increased conductivity was due to a bridge between the dimeric Cu subunits provided by the TCNQ molecules. By inserting unoccupied TCNQ molecular orbital into the HOMO-LUMO gap of HKUST-1, the band gap narrows and a pathway was established for charge transfer between HKUST-1 and TCNQ. These conducting porous MOF films has the potential for practical applications in conformal electronic devices, reconfigurable electronics, and sensors.

Because of the well-defined anchoring of MOF on the electrodes, oriented MOF films offer huge promise for electrical applications, such as solar cells, photodetectors and storage medium. Very recently, Erickson and coworkers<sup>[104]</sup> demonstrated a thermoelectric material with high Seebeck coefficient and low thermal conductivity. The active material in this device was HKUST-1@TCNQ film, which was prepared at room-temperature by the process of immersing HKUST-1 films with preferred [111] orientation into the TCNQ/methanol solution. The thermoelectric properties of the conducting portion were measured using Peltier temperature control elements to create a temperature gradient. A large, positive Seebeck coefficient was obtained at room temperature, which can be explained by the hole transport in the MOF valence band. The thermal conductivity measured by time dependent thermoreflectance (TDTR) was found to be low in this system, which possibly owing to the presence of disorder, as suggested by molecular dynamics simulations. The new material opens up a new avenue for the future development of thermoelectric materials.

Pan and coworkers<sup>[105]</sup> fabricated a flexible MOF device which exhibits promising memory performance. By deposition HKUST-1 onto the flexible gold-coated polyethylene terephthalate (PET) substrates using liquid phase epitaxy approach, a high quality MOF nanofilm was fabricated

(Figure 19a). The high quality HKUST-1 nanofilm was grown along [111] direction which was verified by X-ray

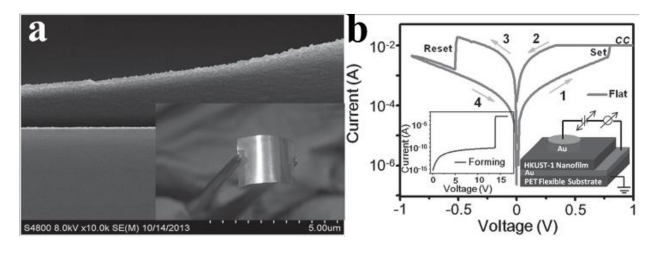


**Figure 19.** (a) digital photograph of the HKUST-1 nanofilm grown on the flexible Au/PET substrate. The thickness of the Au/PET substrate is 7 mil (or  $\approx$  0.18 mm). (b) Current-voltage characteristics of the Au/HKUST-1/Au/PET flexible device at the flat state. The inset shows the schematic configuration and the forming process of the memory device. [105]

diffraction pattern, Fourier transformed infrared spectrum and Raman spectrum. The solid-state Au/HKUST-1/Au/ thin film device showed uniform and reproducible resistive switching effect. Under the strain of as high as 2.8%, the resistance switching of HKUST-1 nanofilm was obtained over the wide temperature range from -70 to  $+70\,^{\circ}$ C. The conductive atomic force microscopic and depth-profiling X-ray photoelectron spectroscopic analysis suggested that the formation of highly conducting filaments caused by electric field-induced migration of the Cu<sup>2+</sup> ions and pyrolysis of the trimesic acid linkers may be the possible origin for the resistance switching effects. This MOF nanofilm has great potential as an information storage medium for future wearable electronic devices.

Liu and coworkers fabricated the prototype organic photovoltaic device (Figure 20) based on the oriented crystalline porphyrin film fabricated by liquid-phase epitaxy method. [106, 107] Since the thin film is highly porous, ordered and oriented, it reveals a small dispersion of occupied and unoccupied bands leading to the formation of a small indirect band gap which can substantially improve device performance (Indirect band gaps support fast and highly efficient charge separation and strongly suppress charge-carrier recombination). Compared with crystalline organic semiconductors, the oriented crystalline porphyrin film exhibited superior photophysical properties, including large charge-carrier mobility and unusually large charge-carrier generation efficiency. Therefore, this photovoltaic device based on Pd porphyrin Zn-SURMOF behaved a remarkable efficiency which showed an open-circuit voltage of 0.7 V, a short circuit current density of 0.71 mA cm<sup>-2</sup>, a fill factor of 0.65 and the efficiency of 0.45%. By loading the pores within the frameworks with electroactive molecules, the oriented crystalline MOF films have the opportunity to achieve much higher

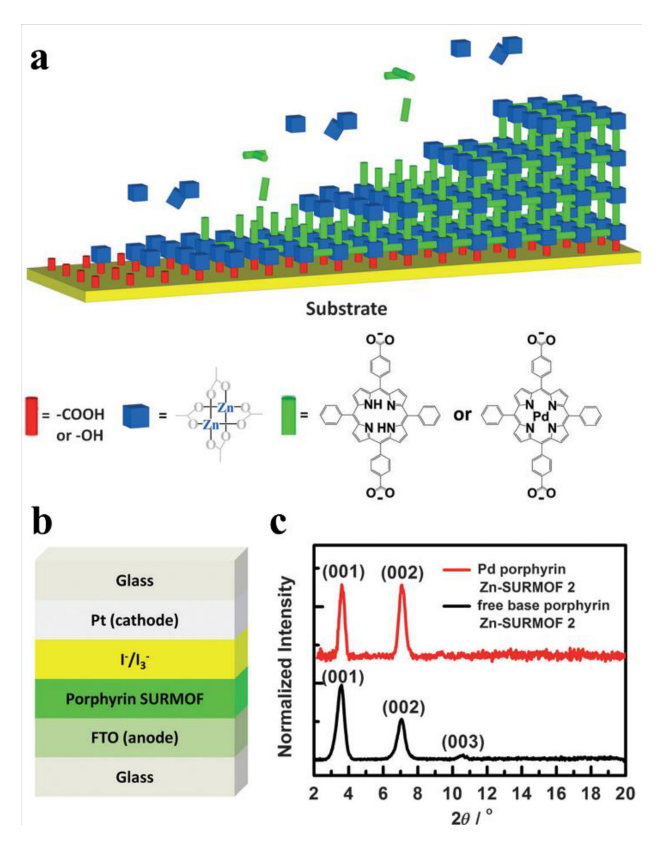


**Figure 20.** SURMOF preparation and characterization. (a) Idealized schematic description of liquid-phase epitaxy deposition process on functionalized substrates in a layer-by-layer fashion with zinc acetate and free-base porphyrin and Pd porphyrin organic linkers. (b) Architecture of porphyrin SURMOF based photovoltaic device. (c) Out of plane X-ray diffraction data of free-base porphyrin Zn-SURMOF 2 and Pd porphyrin Zn-SURMOF 2 grown on FTO glass substrates. [106]

performances (such as a better charge separation) in electrical devices in the future.

Besides the electrical conducting properties, the oriented crystalline MOF thin films also show excellent proton-conducting

property. Xu et. al. [108] studied the proton-conducting property of highly oriented MOF film which was fabricated by "modular assembly" method (Figure 21). The Cu-TCPP nanosheets with high aspect ratio (thickness ~15 nm, diameter ~400 nm) were deposited as a channel between the patterned Cr/Au electrodes on a SiO<sub>2</sub>/Si wafer. Alternating current impedance measurements showed that the proton conductivity of this film increased dramatically with the increasing relative humidity (RH), and reaching  $3.9 \times 10^{-3}$  S cm<sup>-1</sup> at 98 % RH and 25 °C. This value is quite high among hydrated MOFs and is comparable with the proton conductivity of acid-impregnated MOF materials. Although the surface of nanocrystal was important for the proton transport, the numerous dangling functional groups within the 2-D

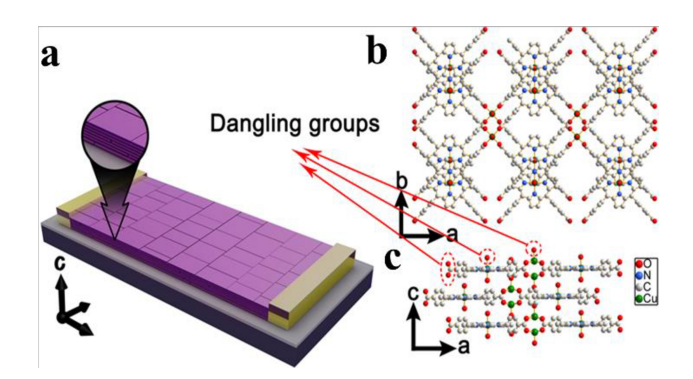


**Figure 21.** Schematic of the nanosheet-constructed MOF nanofilm for electrical measurement (a) and the modeled crystal structure of the MOF nanofilm (b and c). All H atoms are omitted for clarity. <sup>[108]</sup> Copyright 2013, American Chemical Society.

sheet might play dominant role in constructing the proton pathway. This work will be beneficial for the utilization of MOF material in micropower systems, such as microfuel cells and microbatteries.

### 4. Conclusion and Outlook

This review illustrates some fabrication methods of MOF thin films with highly crystalline orientation and emerging opportunities for using them in different applications. For wider application of micro- and nano- device architectures, variety of MOF thin film fabrication techniques had been developed over the past few years. The liquid-phase epitaxy, LB-LbL and "modular assembly" methods are the particularly noteworthy approaches, by which the growth direction and the thickness of thin films can be controlled accurately. Further investigation is urgently required for expanding the use of these methods and developing the generic processing techniques suitable for a broad range of MOF films. Controllable preparation methods of single-crystal MOF thin films and free-standing MOF thin films with highly orientation should also be also attended. More fundamental needs are still recommended in oriented MOF films, including fast wide-area growth, defect control, and precise lithographic patterning, chemical and thermal stability as well as the adhesion between films and the corresponding substrates, which are very important for fabricating MOF thin filmbased devices.

It is encouraging that the oriented MOF thin films play the active roles in recent demonstration of several applications. Combination of long-range order and synthetic flexibility, the MOF films with highly crystalline and orientation show a wide range of tunable properties in functional devices. The studies of optical properties, selective adsorption/separation, electrical properties, sensors and electrical devices has been exhibited. Subsequent focuses on the possible applications of MOF thin film with different orientation need to be expanded. The fabrication of various kinds of functional MOF films, such as conductive films and optical films, are also an imperative task for practical applications. It is understatement to predict that the highly ordered MOF films will have a promising future for the MOF-based devices.

### Acknowledgements

The authors gratefully thank current co-workers, Dr. Mingshui Yao, Dr. Guange Wang, Dr. Bhaskar Nath, Dr. Guodong Wu, Wenhua Li, Weihua Deng, Meng Tian, Jingwei Xiu, Jiahong Huang, Ying Zang, Yanzhou Li and Xiaojing Lv for their selfless assistance. The work was financially supported by National Natural Science Foundation of China (No. 51402293) the Natural Science Foundation of Fujian Province, China (No.2016 J05053).

- H. Li, M. Eddaoudi, M. O'Keeffe, O. M. Yaghi, *Nature* 1999, 402, 276–279.
- [2] O. M. Yaghi, M. O'Keeffe, N. W. Ockwig, H. K. Chae, M. Eddaoudi, J. Kim, *Nature* 2003, 423, 705–714.
- [3] S. Kitagawa, R. Kitaura, S. i. Noro, *Angew. Chem. Int. Ed.* **2004**, *43*, 2334–2375.
- [4] M. Kurmoo, Chem. Soc. Rev. 2009, 38, 1353-1379.
- [5] G. Férey, Chem. Soc. Rev. 2008, 37, 191-214.
- [6] L. J. Murray, M. Dincă, J. R. Long, Chem. Soc. Rev. 2009, 38, 1294–1314.
- [7] J. C. Tan, A. K. Cheetham, Chem. Soc. Rev. 2011, 40, 1059–1080.
- [8] J.-R. Li, J. Sculley, H.-C. Zhou, Chem Rev. 2011, 112, 869–932.
- [9] L. E. Kreno, K. Leong, O. K. Farha, M. Allendorf, R. P. Van Duyne, J. T. Hupp, *Chem Rev.* 2011, 112, 1105–1125.
- [10] J. Lee, O. K. Farha, J. Roberts, K. A. Scheidt, S. T. Nguyen, J. T. Hupp, *Chem. Soc. Rev.* **2009**, *38*, 1450–1459.
- [11] J. An, S. J. Geib, N. L. Rosi, J. Am. Chem. Soc. 2009, 131, 8376–8377.
- [12] M. Alvaro, E. Carbonell, B. Ferrer, F. X. Llabrés i Xamena, H. Garcia, Chem.-Eur. J. 2007, 13, 5106–5112.
- [13] J. M. Taylor, K. W. Dawson, G. K. Shimizu, J. Am. Chem. Soc. 2013, 135, 1193–1196.
- [14] A. Betard, R. A. Fischer, Chem Rev. 2012, 112, 1055-83.
- [15] V. Stavila, A. Talin, M. Allendorf, Chem. Soc. Rev. 2014, 43, 5994–6010.
- [16] L. Heinke, M. Tu, S. Wannapaiboon, R. A. Fischer, C. Wöll, Microporous Mesoporous Mater. 2015, 216, 200–215.
- [17] E. Biemmi, C. Scherb, T. Bein, J. Am. Chem. Soc. 2007, 129, 8054–8055.
- [18] D. Zacher, A. Baunemann, S. Hermes, R. A. Fischer, J. Mater. Chem. 2007, 17, 2785–2792.

- [19] O. Shekhah, H. Wang, S. Kowarik, F. Schreiber, M. Paulus, M. Tolan, C. Sternemann, F. Evers, D. Zacher, R. A. Fischer, J. Am. Chem. Soc. 2007, 129, 15118–15119.
- [20] R. Makiura, S. Motoyama, Y. Umemura, H. Yamanaka, O. Sakata, H. Kitagawa, *Nature Mater.* 2010, 9, 565–571.
- [21] G. Xu, T. Yamada, K. Otsubo, S. Sakaida, H. Kitagawa, J. Am. Chem. Soc. 2012, 134, 16524–16527.
- [22] D. Zacher, O. Shekhah, C. Woll, R. A. Fischer, Chem. Soc. Rev. 2009, 38, 1418–1429.
- [23] A. Bétard, R. A. Fischer, Chem. Rev. 2011, 112, 1055– 1083.
- [24] B. Liu, R. A. Fischer, Sci China Chem. 2011, 54, 1851– 1866.
- [25] O. Shekhah, J. Liu, R. Fischer, C. Wöll, Chem. Soc. Rev. 2011, 40, 1081–1106.
- [26] M, Tu, S. Wannapaiboon, R. A. Fischer, *Inorg. Chem. Front.* 2014, 1, 442–463.
- [27] L. Heinke, M. Tu, S. Wannapaiboon, R. A. Fischer, C. Wöll, Microporous Mesoporous Mater. 2015, 216, 200–215.
- [28] K. Otsubo, H. Kitagawa, APL Mater. 2014, 2, 124105.
- [29] J. L. Zhuang, A. Terfort, C. Wöll, Coord. Chem. Rev. 2016, 307, 391–424.
- [30] C. Scherb, A. Schödel, T. Bein, Angew. Chem. Int. Ed. 2008, 47,5777-5779.
- [31] C. Scherb, R. Koehn, T. Bein, J. Mater. Chem. 2010, 20, 3046–3051.
- [32] A. Schoedel, C. Scherb, T. Bein, Angew. Chem. Int. Ed. 2010, 49, 7225–7228.
- [33] F. Hinterholzinger, C. Scherb, T. Ahnfeldt, N. Stock, T. Bein, *Phys Chem Chem Phys.* **2010**, *12*, 4515–4520.
- [34] O. Shekhah, A. Cadiau, M. Eddaoudi, CrystEngComm 2015, 17, 290–294.
- [35] O. Shekhah, H. Wang, D. Zacher, R. A. Fischer, C. Wöll, Angew. Chem. Int. Ed. 2009, 48, 5038–5041.
- [36] O. Shekhah, H. Wang, M. Paradinas, C. Ocal, B. Schüpbach, A. Terfort, D. Zacher, R. A. Fischer, C. Wöll, Nature Mater. 2009, 8, 481–484.
- [37] H. Gliemann, C. Wöll, Materials Today 2012, 15, 110– 116.
- [38] O. Shekhah, K. Hirai, H. Wang, H. Uehara, M. Kondo, S. Diring, D. Zacher, R. Fischer, O. Sakata, S. Kitagawa, *Dalton Trans.* 2011, 40, 4954–4958.
- [39] H. K. Arslan, O. Shekhah, J. Wohlgemuth, M. Franzreb, R. A. Fischer, C. Wöll, *Adv. Funct. Mater.* 2011, 21, 4228– 4231.
- [40] Z.-G. Gu, A. Pfriem, S. Hamsch, H. Breitwieser, J. Wohlgemuth, L. Heinke, H. Gliemann, C. Wöll, *Micro-porous Mesoporous Mater.* 2015, 211, 82–87.
- [41] V. Chernikova, O. Shekhah, M. Eddaoudi, ACS Appl. Mater. Interfaces 2016, 8, 20459–20464
- [42] K. Kanaizuka, R. Haruki, O. Sakata, M. Yoshimoto, Y. Akita, H. Kitagawa, J. Am. Chem. Soc. 2008, 130, 15778– 15779.
- [43] R. A. Fischer, C. Wöll, Angew. Chem. Int. Ed. 2009, 48, 6205–6208.
- [44] H. Furukawa, K. E. Cordova, M. O'Keeffe, O. M. Yaghi, Science 2013, 341, 1230444.

- [45] K. Yusenko, M. Meilikhov, D. Zacher, F. Wieland, C. Sternemann, X. Stammer, T. Ladnorg, C. Wöll, R. A. Fischer, *CrystEngComm* **2010**, *12*, 2086–2090.
- [46] V. Stavila, C. Schneider, C. Mowry, T. R. Zeitler, J. A. Greathouse, A. L. Robinson, J. M. Denning, J. Volponi, K. Leong, W. Quan, M. Tu, R. A. Fischer, M. D. Allendorf, Adv. Funct. Mater. 2016, 26, 1699–1707.
- [47] X-J Yu, J-L Zhuang, J. Scherr, T. Abu-Husein, A. Terfort, Angew. Chem. Int. Ed. 2016, 55, 1–6.
- [48] H. K. Arslan, O. Shekhah, D. F. Wieland, M. Paulus, C. Sternemann, M. A. Schroer, S. Tiemeyer, M. Tolan, R. A. Fischer, C. Wöll, J. Am. Chem. Soc. 2011, 133, 8158–8161.
- [49] B. Liu, O. Shekhah, H. K. Arslan, J. Liu, C. Wöll, R. A. Fischer, Angew. Chem. Int. Ed. 2012, 51, 807–810.
- [50] K. Otsubo, T. Haraguchi, O. Sakata, A. Fujiwara, H. Kitagawa, J. Am. Chem. Soc. 2012, 134, 9605–9608.
- [51] R. Makiura, H. Kitagawa, Eur. J. Inorg. Chem. 2010, 2010, 3715–3724.
- [52] S. Motoyama, R. Makiura, O. Sakata, H. Kitagawa, J. Am. Chem. Soc. 2011, 133, 5640–5643.
- [53] R. Makiura, O. Konovalov, *Dalton Trans.* 2013, 42, 15931–15936.
- [54] R. Makiura, O. Konovalov, Sci Rep. 2013, 3, 2506.
- [55] V. Rubio-Giménz, S. Tatay, F. Volatron, F. J. Martínez-Casado, C. Martí-Gastaldo, E. Coronado, J. Am. Chem. Soc. 2016, 138, 2576–2584.
- [56] R. Dong, M. Pfeffermann, H. Liang, Z. Zheng, X. Zhu, J. Zhang, X. Feng, Angew. Chem. Int. Ed. 2015, 54, 12058– 12063.
- [57] O. Shekhah, J. Liu, R. Fischer, C. Wöll, Chem. Soc. Rev. 2011, 40, 1081–1106.
- [58] D. Bradshaw, A. Garai, J. Huo, Chem. Soc. Rev. 2012, 41, 2344–2381.
- [59] M. Shah, M. C. McCarthy, S. Sachdeva, A. K. Lee, H.-K. Jeong, *Ind. Eng. Chem. Res.* 2012, 51, 2179–2199.
- [60] P. Horcajada, C. Serre, D. Grosso, C. Boissiere, S. Perruchas, C. Sanchez, G. Férey, Adv. Mater. 2009, 21, 1931–1935.
- [61] A. Demessence, P. Horcajada, C. Serre, C. Boissière, D. Grosso, C. Sanchez, G. Férey, *Chem Commun.* 2009, 7149–7151.
- [62] H. Guo, Y. Zhu, S. Qiu, J. A. Lercher, H. Zhang, Adv. Mater. 2010, 22, 4190–4192.
- [63] E. Redel, Z. Wang, S. Walheim, J. Liu, H. Gliemann, C. Wöll, Appl Phys Lett. 2013, 103, 091903.
- [64] W. Zhang, G. Lu, S. Li, Y. Liu, H. Xu, C. Cui, W. Yan, Y. Yang, F. Huo, Chem Commun. 2014, 50, 4296–4298.
- [65] I. Hod, W. Bury, D. M. Karlin, P. Deria, C. W. Kung, M. J. Katz, M. So, B. Klahr, D. Jin, Y. W. Chung, Adv. Mater. 2014, 26, 6295–6300.
- [66] M. C. So, G. P. Wiederrecht, J. E. Mondloch, J. T. Hupp, O. K. Farha, *Chem Commun.* 2015, *51*, 3501–3510.
- [67] H. C. Streit, M. Adlung, O. Shekhah, X. Stammer, H. K. Arslan, O. Zybaylo, T. Ladnorg, H. Gliemann, M. Franzreb, C. Wöll, ChemPhysChem. 2012, 13, 2699–2702.

- [68] M. C. So, S. Jin, H.-J. Son, G. P. Wiederrecht, O. K. Farha, J. T. Hupp, J. Am. Chem. Soc. 2013, 135, 15698– 15701.
- [69] B. Liu, M. Ma, D. Zacher, A. Bétard, K. Yusenko, N. Metzler-Nolte, C. Wöll, R. A. Fischer, J. Am. Chem. Soc. 2011, 133, 1734–1737.
- [70] L. Heinke, M. Cakici, M. Dommaschk, S. Grosjean, R. Herges, S. Bräse, C. Wöll, ACS nano. 2014, 8, 1463–1467.
- [71] G. Lu, J. T. Hupp, J. Am. Chem. Soc. 2010, 132, 7832–7833.
- [72] M. D. Allendorf, R. J. Houk, L. Andruszkiewicz, A. A. Talin, J. Pikarsky, A. Choudhury, K. A. Gall, P. J. Hesketh, J. Am. Chem. Soc. 2008, 130, 14404–14405.
- [73] I. Ellern, A. Venkatasubramanian, J.-H. Lee, P. Hesketh, V. Stavila, A. Robinson, M. Allendorf, *Micro Nano Lett.* 2013, 8, 766–769.
- [74] B. Liu, M. Tu, R. A. Fischer, Angew. Chem. Int. Ed. 2013, 52, 3402–3405.
- [75] M. Tu, S. Wannapaiboon, R. A. Fischer, *Dalton Trans.* 2013, 42, 16029–16035.
- [76] M. Meilikhov, S. Furukawa, K. Hirai, R. A. Fischer, S. Kitagawa, Angew. Chem. Int. Ed. 2013, 52, 341–345.
- [77] M. Tu, R. A. Fischer, J. Mater. Chem. A 2014, 2, 2018– 2022
- [78] S. Wannapaiboon, M. Tu, R. A. Fischer, Adv. Funct. Mater. 2014, 24, 2696–2705.
- [79] Z. Wang, H. Sezen, J. Liu, C. Yang, S. E. Roggenbuck,
  K. Peikert, M. Fröba, A. Mavrantonakis, B. Supronowicz,
  T. Heine, Microporous Mesoporous Mater. 2015, 207, 53–60.
- [80] O. Shekhah, M. Eddaoudi, Chem Commun. 2013, 49, 10079–10081.
- [81] T. Haraguchi, K. Otsubo, O. Sakata, A. Fujiwara, H. Kitagawa, *Inorg. Chem.* 2015, 54, 11593–11595.
- [82] T. Haraguchi, K. Otsubo, O. Sakata, S. Kawaguchi, A. Fujiwarad, H. Kitagawa, Chem. Commun., 2016, 52, 6017–6020.
- [83] S. Sakaida, K. Otsubo, O. Sakata, C. Song, A. Fujiwara, M. Takata, H. Kitagawa, *Nature Chem.* 2016, 8, 377–383.
- [84] S. Qiu, M. Xue, G. Zhu, Chem. Soc. Rev. 2014, 43, 6116–6140.
- [85] Y. Liu, N. Wang, L. Diestel, F. Steinbach, J. Caro, Chem Commun. 2014, 50, 4225–4227.
- [86] Y. Liu, G. Zeng, Y. Pan, Z. Lai, J Memb Sci. 2011, 379, 46–51.
- [87] A. Huang, W. Dou, J. r. Caro, J. Am. Chem. Soc. 2010, 132, 15562–15564.
- [88] Y. Mao, H. Huang, W. Cao, J. Li, L. Sun, X. Jin, X. Peng, *Chem Commun.* **2013**, *49*, 5666–5668.
- [89] Y. Mao, B. Su, W. Cao, J. Li, Y. Ying, W. Ying, Y. Hou, L. Sun, X. Peng, ACS Appl. Mater. Interfaces 2014, 6, 15676–15685.
- [90] B. A. Al-Maythalony, O. Shekhah, R. Swaidan, Y. Belmabkhout, I. Pinnau, M. Eddaoudi, J. Am. Chem. Soc. 2015, 137, 1754–1757.

- [91] A. Huang, Y. Chen, N. Wang, Z. Hu, J. Jiang, J. Caro, Chem Commun. 2012, 48, 10981–10983.
- [92] S. Sorribas, P. Gorgojo, C. Téllez, J. Coronas, A. G. Livingston, J. Am. Chem. Soc. 2013, 135, 15201–15208.
- [93] Y. S. Li, H. Bux, A. Feldhoff, G. L. Li, W. S. Yang, J. Caro, Adv. Mater. 2010, 22, 3322–3326.
- [94] A. J. Bons, P. D. Bons, Microporous Mesoporous Mater. 2003, 62, 9-16.
- [95] Y. S. Li, F. Y. Liang, H. Bux, A. Feldhoff, W. S. Yang, J. Caro, Angew. Chem. Int. Ed. 2010, 49, 548–551.
- [96] H. Bux, A. Feldhoff, J. Cravillon, M. Wiebcke, Y.-S. Li, J. Caro, Chem Mater. 2011, 23, 2262–2269.
- [97] H. Bux, F. Liang, Y. Li, J. Cravillon, M. Wiebcke, J. r. Caro, J. Am. Chem. Soc. 2009, 131, 16000–16001.
- [98] Z. G. Gu, J. Bürck, A. Bihlmeier, J. Liu, O. Shekhah, P. G. Weidler, C. Azucena, Z. Wang, S. Heissler, H. Gliemann, *Chem.-Eur. J.* 2014, 20, 9879–9882.
- [99] Z.-G. Gu, S. Grosjean, S. Bräse, C. Wöll, L. Heinke, Chem Commun. 2015, 51, 8998–9001.
- [100] M. Tsotsalas, J. Liu, B. Tettmann, S. Grosjean, A. Shahnas, Z. Wang, C. Azucena, M. Addicoat, T. Heine, J. Lahann, J. Am. Chem. Soc. 2013, 136, 8–11.
- [101] V. Mugnaini, M. Tsotsalas, F. Bebensee, S. Grosjean, A. Shahnas, S. Bräse, J. Lahann, M. Buck, C. Wöll, Chem Commun. 2014, 50, 11129–11131.
- [102] A. Dragässer, O. Shekhah, O. Zybaylo, C. Shen, M. Buck, C. Wöll, D. Schlettwein, *Chem Commun.* 2012, 48, 663–665.
- [103] A. A. Talin, A. Centrone, A. C. Ford, M. E. Foster, V. Stavila, P. Haney, R. A. Kinney, V. Szalai, F. El Gabaly, H. P. Yoon, *Science* 2014, 343, 66–69.
- [104] K. J. Erickson, F. Léonard, V. Stavila, M. E. Foster, C. D. Spataru, R. E. Jones, B. M. Foley, P. E. Hopkins, M. D. Allendorf, A. A. Talin, Adv. Mater. 2015, 27, 3453–3459.
- [105] L. Pan, Z. Ji, X. Yi, X. Zhu, X. Chen, J. Shang, G. Liu, R. W. Li, Adv. Funct. Mater. 2015, 25, 2677–2685.
- [106] J. Liu, W. Zhou, J. Liu, I. Howard, G. Kilibarda, S. Schlabach, D. Coupry, M. Addicoat, S. Yoneda, Y. Tsutsui, T. Sakurai, S. Seki, Z. Wang, P. Lindemann, E. Redel, T. Heine, C. Wöll, Angew. Chem. Int. Ed. 2015, 54, 7441–7445.
- [107] J. Liu, W. Zhou, J. Liu, Y. Fujimori, T. Higashino, H. Imahori, X. Jiang, J. Zhao, T. Sakurai, Y. Hattori, W. Matsuda, S. Seki, S. K. Garlapati, S. Dasgupta, E. Redel, L. Sunag, C. Wöll, J. Mater. Chem. A, 2016, 4, 12739–12747.
- [108] G. Xu, K. Otsubo, T. Yamada, S. Sakaida, H. Kitagawa, J. Am. Chem. Soc. 2013, 135, 7438–7441.

Received: June 26, 2016 Accepted: September 12, 2016 Published online on October 24, 2016